Received: 24 May 2021 | Accepted: 25 August 2021

DOI: 10.1002/prp2.870

ORIGINAL ARTICLE

In vitro investigations into the roles of CYP450 enzymes and drug transporters in the drug interactions of zanubrutinib, a covalent Bruton's tyrosine kinase inhibitor

Heather Zhang[1] | Ying C. Ou[1] | Dan Su[2] | Fan Wang[2] | Lai Wang[2] | Srikumar Sahasranaman[1] | Zhiyu Tang[1]

[1]BeiGene USA, Inc., San Mateo, CA, USA

[2]BeiGene (Beijing) Co., Ltd, Beijing, China

Correspondence
Heather Zhang, Clinical Pharmacology, BeiGene, Ltd., 2955 Campus Drive, Suite 300, San Mateo, CA 94403, USA.
Email: heather.zhang@beigene.com

Funding information
BeiGene, Ltd.

Abstract

Zanubrutinib is a highly selective, potent, orally available, targeted covalent inhibitor (TCI) of Bruton's tyrosine kinase (BTK). This work investigated the in vitro drug metabolism and transport of zanubrutinib, and its potential for clinical drug–drug interactions (DDIs). Phenotyping studies indicated cytochrome P450 (CYP) 3A are the major CYP isoform responsible for zanubrutinib metabolism, which was confirmed by a clinical DDI study with itraconazole and rifampin. Zanubrutinib showed mild reversible inhibition with half maximal inhibitory concentration (IC_{50}) of 4.03, 5.69, and 7.80 μM for CYP2C8, CYP2C9, and CYP2C19, respectively. Data in human hepatocytes disclosed induction potential for CYP3A4, CYP2B6, and CYP2C enzymes. Transport assays demonstrated that zanubrutinib is not a substrate of human breast cancer resistance protein (BCRP), organic anion transporting polypeptide (OATP)1B1/1B3, organic cation transporter (OCT)2, or organic anion transporter (OAT)1/3 but is a potential substrate of the efflux transporter P-glycoprotein (P-gp). Additionally, zanubrutinib is neither an inhibitor of P-gp at concentrations up to 10.0 μM nor an inhibitor of BCRP, OATP1B1, OATP1B3, OAT1, and OAT3 at concentrations up to 5.0 μM. The in vitro results with CYPs and transporters were correlated with the available clinical DDIs using basic models and mechanistic static models. Zanubrutinib is not likely to be involved in transporter-mediated DDIs. CYP3A inhibitors and inducers may impact systemic exposure of zanubrutinib. Dose adjustments may be warranted depending on the potency of CYP3A modulators.

Abbreviations: A-B, apical-to-basolateral; ACN, acetonitrile; AUC, area under the plasma concentration versus time curve; AUCR, ratio of AUC; B-A, basolateral-to-apical; BCRP, breast cancer resistance protein; BTK, Bruton's tyrosine kinase; CLL, chronic lymphocytic leukemia; C_{max}, maximum plasma concentration; CYP, cytochrome P450; DDI, drug–drug interaction; DMEM, Dulbecco's Modified Eagle's Medium; EC_{50}, concentration supporting half-maximal enzyme induction; E_{max}, maximum fold induction; F_g, the fraction available after intestinal metabolism; F_m, the fraction of metabolism by the specific CYP; f_{up}, free plasma protein binding; HER2, human epidermal growth factor receptor 2; HLM, human liver microsomes; IC_{50}, half maximal inhibitory concentration; K_i, the reversible inhibition constant; LC-MS/MS, liquid chromatography-tandem mass spectrometry; LFY, Lucifer Yellow; MDCK, Madin–Darby canine kidney; MDR1, multidrug resistance mutation 1; OAT, organic anion transporter; OATP, organic anion transporting polypeptide; OCT, organic cation transporter; P_{app}, apparent permeability; P-gp, P-glycoprotein; PK, pharmacokinetics; R/R, relapsed/refractory; rCYP, recombinant CYP; SLC, solute carrier; SLL, small lymphocytic lymphoma; TCI, targeted covalent inhibitor; UDPGA, UDP glucuronic acid; WM, Waldenström macroglobulinemia.

KEYWORDS
BTK inhibitor, CYP induction, CYP inhibition, drug metabolism, transporter inhibition, transporter substrate

1 | INTRODUCTION

B-cell receptor signaling is not only essential for normal B-cell development but is also implicated in the survival and proliferation of malignant B cells. Bruton's tyrosine kinase (BTK), a Tec family kinase expressed in B cells, myeloid cells, mast cells, and platelets, plays an integral role in the B-cell receptor signaling responsible for the proliferation and survival of malignant B cells.[1,2] Irreversible BTK inactivation was established as a valuable clinical target for the treatment of B-cell malignancies by ibrutinib, the first-in-class BTK inhibitor. Ibrutinib has become a standard of care in chronic lymphocytic leukemia/small lymphocytic lymphoma (CLL/SLL), mantle cell lymphoma (MCL), and Waldenström macroglobulinemia (WM).[3] However, adverse effects of ibrutinib therapy include bleeding and atrial fibrillation, which were postulated to involve off-target activity against other Tec and Src family kinases.[4]

Zanubrutinib (Brukinsa®, BGB-3111) is a highly selective, potent, orally available targeted covalent inhibitor (TCI) of BTK that has received approval for the treatment of WM and relapsed/refractory (R/R) MCL and marginal zoone lymphoma by the United States Food and Drug Administration (FDA), for the treatment of R/R CLL/SLL, MCL, and WM by the China National Medical Products Administration, for the treatment of WM and R/R MCL in Canada, and for the treatment of R/R MCL in Brazil, the United Arab Emirates, Israel, and Chile.[5] Zanubrutinib has demonstrated improved selectivity over ibrutinib for the inhibition of BTK versus other receptor tyrosine kinases.[6,7] The improved selectivity for BTK may result in a lower incidence and severity of off-target toxicities compared with ibrutinib. The recommended phase 2 and 3 dose is 160 mg orally (PO) twice daily (BID). Emerging clinical data have shown that zanubrutinib is associated with favorable pharmacokinetics (PK) and a high objective response rate with a low incidence of major toxicities in patients with B-cell malignancies, including WM, MCL, and CLL.[8–10]

The management of drug–drug interactions (DDIs) for cancer therapies is challenging because the major mechanisms of DDIs for anticancer drugs involve metabolic enzymes, ATP-binding cassette efflux transporters, and solute carrier (SLC) uptake transporters. In patients with B-cell malignancies, concurrent use of ibrutinib and acalabrutinib with strong CYP3A inhibitors, such as azole antifungals (e.g., voriconazole, posaconazole), is mostly prohibited.[3,11–13] Moreover, a cancer drug itself can be a potent enzyme inhibitor or inducer and will therefore impact the systemic exposure of concomitant enzyme substrates. For example, idelalisib is a potent CYP3A inhibitor that can increase the exposure of midazolam by 5.15-fold.[14] In addition to metabolic enzymes, drug transporters can also influence the PK of drugs.[9,15,16] An overlap in substrate and inhibitor specificity for P-gp and for CYP3A has been observed for many drugs.[16] A drug's status as a P-gp or BCRP substrate impacts its entry into restricted tissues, such as brain or placenta. Alternatively, absorption and elimination of P-gp or BCRP substrates can be affected through the modulation of these transporters. For example, the anticancer drug neratinib, a P-gp inhibitor, increased mean digoxin maximum plasma concentration (C_{max}) by 54% and the area under the plasma concentration versus time curve (AUC) of digoxin by 32% in healthy subjects.[17] Statins, substrates of OATP, are commonly used with cancer drugs and the AUC for statins can increase to as high as 10-fold when co-administered with potent OATP inhibitors.[18] Therefore, the metabolism and transport-mediated DDI potential of zanubrutinib need to be thoroughly investigated during development.

Zanubrutinib is under investigation for administration with a combination of a wide variety of other drugs, including agents for non-cancer–related comorbidities. The objective of this study was to investigate the mechanisms of the potential roles of metabolizing enzymes and transporters associated with zanubrutinib disposition and DDIs and to provide an understanding of the relationship between in vitro investigation and clinical drug interaction.

2 | MATERIALS AND METHODS

The test article zanubrutinib (BGB-3111) and the standard BGB-7941 for metabolite M5 were provided by BeiGene Co., Ltd. All other reagents and chemicals were obtained from commercial sources. Metabolite profiling in pooled liver microsomes (BD Biosciences), CYP phenotyping, CYP inhibition and induction, and P-gp inhibition assays were conducted by 3D BioOptima. Contract labs and vendors for other assays are described in their respective sections. After incubation of zanubrutinib in in vitro systems, the reaction was terminated by the addition of acetonitrile (ACN) spiked with glibenclamide as an internal standard, followed by centrifugation. The supernatant was diluted with water and subjected to liquid chromatography-tandem mass spectrometry (LC-MS/MS) analysis.

2.1 | In vitro metabolism

In vitro metabolism of zanubrutinib was assessed in mouse, rat, dog, and human liver microsomes. Zanubrutinib (10 μM) was incubated for 60 min with liver microsomes (1 mg/ml), NADPH (1 mM), UDP glucuronic acid (UDPGA) (1 mM), $MgCl_2$ (3 mM), alamethicin (5 μg/mg), and phosphate buffer (100 mM, pH 7.4). Reconstituted samples were submitted for UV detection, and LC-MS and LC-MS/MS analyses.

2.2 | Identification of enzymes metabolizing zanubrutinib

Zanubrutinib phenotyping of CYPs was assessed with human liver microsomes (HLMs) with specific inhibitors and recombinant CYPs (rCYPs; Corning). Zanubrutinib (1 μM) was incubated with pooled HLM (0.5 mg/ml) and NADPH (1 mM) for 30 min in the absence or presence of isoform-selective inhibitors (0.2 μM α-naphthoflavone for CYP1A2, 2 μM clopidogrel for CYP2B6, 8 μM montelukast for CYP2C8, 5 μM sulfaphenazole for CYP2C9, 30 μM nootkatone for CYP2C19, 2 μM quinidine for CYP2D6, 1 μM ketoconazole for CYP3A) and isoform-selective probe substrates served as positive controls (40 μM phenacetin for CYP1A2, 100 μM bupropion for CYP2B6, 2 μM amodiaquine for CYP2C8, 5 μM diclofenac for CYP2C9, 40 μM S-mephenytoin for CYP2C19, 5 μM dextromethorphan for CYP2D6, 2 μM midazolam for CYP3A).

Zanubrutinib (1 μM) was incubated for 15 min with each rCYP enzyme (rCYP1A2, rCYP2B6, rCYP2C8, rCYP2C9, rCYP2C19, rCYP2D6, and rCYP3A4) at 50 pmol/ml for 30 min with 1 mM NADPH. Isoform-selective probe substrates, 1 μM phenacetin for CYP1A2, 2 μM bupropion for CYP2B6, 2 μM amodiaquine for CYP2C8, 2 μM diclofenac for CYP2C9, 10 μM S-mephenytoin for CYP2C19, 1 μM dextromethorphan for CYP2D6, and 20 μM midazolam for CYP3A4, were used as positive controls.

2.3 | CYP inhibition

CYP inhibition potential was evaluated in NADPH-fortified HLMs (0.1 mg/ml) using CYP probe substrates (same as the positive controls in HLM phenotyping assays; 80 μM testosterone for CYP3A was also used). Zanubrutinib in triplicates (0, 0.274, 0.823, 2.47, 7.41, 22.2, 66.7, and 200 μM) was incubated with each probe for 20 min (CYP1A2), 10 min (CYP2B6), 5 min (CYP2C8), 7 min (CYP2C9), 20 min (CYP2C19), 10 min (CYP2D6), 5 min (CYP3A, midazolam), and 10 min (CYP3A, testosterone). Selective inhibitors in seven concentrations (furafylline for CYP1A2, ticlopidine for CYP2B6, quercetin for CYP2C8, sulfaphenazole for CYP2C9, nootkatone for CYP2C19, quinidine for CYP2D6, and ketoconazole for CYP3A) served as positive controls. Probe substrate metabolites were analyzed by LC-MS/MS and ratios of analytes to internal standard peak area ratios were calculated. IC_{50} values were calculated by nonlinear regression analyses of data using the Hill equation.[19]

2.4 | Time-dependent CYP inhibition

Zanubrutinib (10 μM) or vehicle in triplicates was pre-incubated with NADPH-fortified HLMs at 1.0 mg/ml for CYP1A2, CYP2B6, CYP2C8, CYP2C9, CYP2C19, CYP2D6, or HLMs at 0.5 mg/ml for CYP3A for 30 min. The HLM mixture was diluted 10-fold to 0.1 mg/ml (20-fold to 0.025 mg/ml for CYP3A) in buffered solution containing a CYP substrate, which was the same as the reversible inhibition assay except 50 μM midazolam was used for CYP3A. The incubation was continued for 20 min for CYP1A2 and CYP2C19, 10 min for CYP2B6 and CYP2D6, 7 min for CYP2C9, 5 min for CYP2C8, and 1.5 min for CYP3A activities. Verapamil served as a positive control. Percent CYP activity loss of a specific CYP was calculated by the following equation.

$$\text{Activity loss} = \left(\frac{A \text{ with drug}}{A \text{ with vehicle}}\right) \text{at } t0 - \left(\frac{A \text{ with drug}}{A \text{ with vehicle}}\right) \text{at } t30\ min,$$

where A is the mean response of the metabolite of a CYP probe; $t0$: no preincubation; $t30$: preincubation for 30 min.

2.5 | CYP induction

Induction of CYP1A2, CYP2B6, and CYP3A enzymes by zanubrutinib in human hepatocytes was evaluated in XBL Inc. Cryopreserved human hepatocytes from three donors and media were purchased from Celsis In Vitro. Hepatocytes were treated with zanubrutinib (0.3, 3, or 30 μM), or a positive control (omeprazole at 50 μM for CYP1A2, phenobarbital at 1000 μM for CYP2B6, or rifampin at 25 μM for CYP3A), or the vehicle medium for 2 days. After culture, total mRNA was extracted, and the RNA content was measured using an ultra-micro spectrophotometer and the RNA was then reverse transcribed into cDNA. Cycle thresholds of CYP1A2, CYP2B6, and CYP3A DNA were quantified using a fluorescence quantitative PCR kit (Takara Bio). CYP induction was calculated using a standard ΔΔCT method.[20] The cells were incubated with 50 μM of CYP1A2 probe phenacetin, CYP2B6 probe bupropion, or CYP3A probe testosterone for 1 h to assess CYP activities. The probe metabolites were analyzed by LC-MS/MS.

Induction of CYP2C8, CYP2C9, and CYP2C19 enzymes by zanubrutinib in human hepatocytes was evaluated in WuXi AppTec. Cryopreserved human hepatocytes from three donors and media were from BioIVT. Both mRNA expression levels and enzymatic activities were assessed for CYP2C8 and CYP2C9 induction. For CYP2C19, only enzymatic activity was reported as the mRNA level did not respond to positive control rifampin. Human hepatocytes were treated for 3 days with zanubrutinib (0.3, 3, and 30 μM) and rifampin (25 μM). At the end of incubation, the cells were incubated with CYP2C8 probe amodiaquine (20 μM), CYP2C9 probe diclofenac (40 μM), and CYP2C19 probe S-mephenytoin (80 μM) for 1 hour to assess CYP activities. The probe metabolites were analyzed by LC-MS/MS.

2.6 | P-gp transportation and inhibition

The P-gp status of zanubrutinib was evaluated in ChemPartner (Shanghai, China) using the Madin–Darby canine kidney (MDCK) cell lines transfected with multidrug resistance gene 1 (MDR1). MDCK-MDR1 cells were obtained from the Netherlands Cancer Institute

(Amsterdam, Netherlands). The MDCK-MDR1 cells were maintained in Dulbecco's Modified Eagle's Medium (DMEM) for 3–4 days prior to the transport experiments. Lucifer Yellow (LFY) permeability was used to indicate monolayer integrity. Zanubrutinib (1 or 10 μM) transportation was tested with or without 100 μM verapamil in both apical-to-basolateral (A-B) and basolateral-to-apical (B-A) directions at 37°C for 90 min. At the end of incubation, receiver and donor samples were both diluted by assay buffer and analyzed by LC-MS/MS. Bidirectional apparent permeability (P_{app}) of A-B and B-A and the efflux ratios (P_{app} [B-A]/P_{app} [A-B]) were then calculated.[19] Metoprolol (5 μM) and quinidine (5 μM) served as high-permeability negative and positive controls, respectively.

The potential to inhibit P-gp by zanubrutinib (0.5 and 10 μM, triplicates) was evaluated using Caco-2 cells (Committee on Type Culture Collection of Chinese Academy of Sciences, Shanghai, China). Aliquots of passage 29 cells were stored in the cell-freezing medium (fetal bovine serum:DMSO = 9:1, v:v) in liquid nitrogen until use. After 21-day culture on membranes, cell monolayers were used for drug transport assays. The incubations were conducted for 120 min using digoxin (10 μM) as the probe substrate for P-gp. Digoxin was quantified by LC-MS/MS. Elacridar (4 μM) served as a positive control.

2.7 | BCRP transportation and inhibition

The potential of zanubrutinib to be transported by BCRP and to inhibit BCRP was evaluated at the Research Institute for Liver Disease (Shanghai, China) using BCRP inside-out vesicles isolated from Sf9 cells expressing human BCRP (GenoMembrane). In the BCRP transportation assay, zanubrutinib (0.1 or 5.0 μM) or the positive control LFY (10 μM) in triplicates was incubated with BCRP vesicles (1 mg/ml, 0.05 mg) and 4 mM of MgATP (MgAMP for passive transport) for 5 min. Uptake ratio of a compound was determined by ratio of uptake rates (pmol/min/mg protein) in the presence of ATP versus AMP.[21]

In the BCRP inhibition assay, the impact of zanubrutinib (0.05, 0.2, 1.0, or 5.0 μM), positive control novobiocin (500 μM), or buffer vehicle (negative control) in triplicates on LFY uptake with BCRP vesicles was evaluated. The LFY amount was analyzed by fluorescence. The inhibitory potential on BCRP by test articles was described by relative BCRP activity (uptake rate % of negative control).[21]

2.8 | Transportation and inhibition of SLC uptake transporters

The potential of zanubrutinib to be transported by SLC uptake transporters and to inhibit these transporters was evaluated at the Research Institute for Liver Disease (Shanghai, China) using recombinant stable human embryonic kidney 293 (HEK293) cells expressing human OATP1B1, OATP1B3, OCT2, OAT1, and OAT3, which were transfected with empty vector (HEK293-MOCK, negative control) (GenoMembrane). Cells (2×10^5 cells/well) were maintained in DMEM medium supplemented with 10% (v/v) fetal calf serum, penicillin-streptomycin solution (100 U/ml and 0.1 mg/ml), and 0.5 mg/ml of geneticin. In the SLC transportation assays, DMEM media were removed from cells, followed by incubation with triplicates of zanubrutinib (0.1, 0.3, or 5 μM) or positive controls (20 μM estradiol-17-glucuronide for OATP1B1/1B3; 20 μM p-aminohippuric acid for OAT1, 20 μM estrone sulfate for OAT3; 50 μM metformin for OCT2) in transportation buffer for 10 min. Transportation buffer contained 250 mM NaCl, 9.6 mM KCl, 11.2 mM D-(+)-glucose, 2.4 mM $CaCl_2$, 2.4 mM $MgSO_4$, and 590 mM HEPEs. After cell washing, 0.15 mL 1 M NaOH was added to each well to lyse the cells for 30 min, and then neutralized with 0.15 mL 1 M HCl. The content of protein was determined by the Pierce BCA protein assay kit (Thermo Scientific, Waltham, MA, USA). The amount of test article was determined by an LC-MS/MS method. An uptake ratio of compound is calculated by the uptake rate (pmol/min/mg protein) in SLC-overexpressed cells divided by mean uptake rate in HEK293-MOCK cells.[22,23]

In the SLC inhibition assay, triplicates of zanubrutinib (0.05, 0.2, or 5 μM), positive controls (100 μM rifampin for OATP1B1/1B3; 50 μM probenecid for OAT1/3; 500 μM quinidine for OCT2), and vehicle were incubated with respective probe substrates (positive controls in the SLC transportation assay). The net uptake rate is the difference of uptake rates between SLC-overexpressed cells and MOCK cells. The inhibitory potential on SLC transporters by test articles is described by relative activity (net uptake rate % of vehicle).[22]

2.9 | In vivo interaction prediction

The in vivo DDI risk of zanubrutinib as a perpetrator impacting CYPs was predicted using basic model value R_1 for CYP reversible inhibition, $R_{1,gut}$ for CYP3A reversible inhibition in the gastrointestinal tract, R_3 for CYP induction, and mechanistic static model for the net effect of CYP inhibition and induction based on FDA DDI guidance.[24,25] The net effect of DDI was determined by the ratio of AUC (AUCR) of a probe substrate in the presence and absence of zanubrutinib.

$$R_1 = 1 + \frac{I_{max,u}}{K_{iu}},$$

where $I_{max,u}$ is unbound plasma C_{max}, defined as C_{max}* free plasma protein binding ratio (f_{up}). Zanubrutinib mean steady-state concentration of 338 ng/ml following 160 mg BID in the dose-escalation study is used for C_{max} (data on file). f_{up} is 0.0583 based on experimental data. $I_{max,u}$ is determined as 0.42 μM. K_{iu} is the reversible inhibition constant (K_i) based on the unbound inhibitor concentration (IC_{50}/2* fraction of unbound zanubrutinib in liver microsome [$f_{u,inc}$]). $f_{u,inc}$ was estimated as 0.79 from the Hallifax & Houston equation[26] based on a microsomal protein concentration of 0.1 mg protein/ml for CYP reversible inhibition assays and a measured LogP of 4.2 for zanubrutinib.

$$R_{1,gut} = 1 + \frac{I_{gut}}{K_{iu}},$$

where I_{gut} is zanubrutinib intestinal concentration, Dose/250 ml (~1360 μM)

$$R_3 = \frac{1}{1 + \left(d \times \frac{E_{max} \times 10 \times I_{max,u}}{E_{50} + 10 \times I_{max,u}}\right)},$$

where E_{max} is maximum fold induction (control = 0) and EC_{50} is concentration supporting half-maximal enzyme induction; the scaling factor d is assumed to be 1.

E_{max} and EC_{50} of CYP mRNA induction were estimated using the simple E_{max} model with double reciprocal plots of zanubrutinib concentration versus fold induction minus 1 (control = 0).[27]

$$\text{Fold induction} = \frac{E_{max} \times [\text{Drug}]}{EC_{50} + [\text{Drug}]}.$$

In the mechanistic static model,[27,28] AUCR is given by

$$\text{AUCR} = \left(\frac{1}{[A_g \times C_g] \times (1 - F_g) + F_g}\right) x \left(\frac{1}{[A_h \times C_h] \times f_m + (1 - f_m)}\right),$$

where A_h and C_h represent the reversible inhibition and induction of hepatic CYPs, respectively, and A_g and C_g represent the reversible inhibition and induction of intestinal CYPs, respectively. F_g is the fraction available after intestinal metabolism. F_m is the fraction of metabolism by the specific CYP. Time-dependent inhibition is not considered here.

$$\text{Reversible inhibition} \quad A_g = \frac{1}{1 + \frac{[I]_g}{K_{iu}}}, \quad A_h = \frac{1}{1 + \frac{[I]_h}{K_{iu}}},$$

$$\text{Induction} \quad C_g = 1 + \frac{d.E_{max}.[I]_g}{EC_{50} + [I]_g}, \quad C_h = 1 + \frac{d.E_{max}.[I]_h}{EC_{50} + [I]_h},$$

$[I]_h$ and $[I]_g$ represent the free portal vein concentration and gut enterocyte concentration, respectively, which are estimated by

$$I_h = f_{up} \times (C_{max} + (F_a \times F_g \times k_a \times \text{Dose}) / Q_h / R_b),$$
$$I_g = F_a \times k_a \times \text{Dose} / Q_{en}.$$

Q_{en}: blood flow through enterocytes (18 L/h); Q_h: hepatic blood flow (97 L/h)[24]; for zanubrutinib, k_a (first-order absorption rate constant): 0.526 estimated from population PK[29]; F_a (fraction absorbed) 0.70 estimated from a human mass balance study; F_g: 0.44 estimated from physiologically based PK (PBPK) modeling[30]; R_b (the human blood-to-plasma ratio): 0.804 from measurement.

2.10 | Nomenclature of targets and ligands

Key protein targets and ligands in this article are hyperlinked to corresponding entries in http://www.guidetopharmacology.org, the common portal for data from the IUPHAR/BPS Guide to PHARMACOLOGY[31] and are permanently archived in the Concise Guide to PHARMACOLOGY 2019/20.[32]

3 | RESULTS

3.1 | In vitro metabolism

After 60-min incubation with cofactors NADPH and UDPGA, zanubrutinib was extensively metabolized in mouse, rat, dog, monkey, and HLMs; a total of 11 metabolites (M1–M11) were found (see Figure 1). Of these, 10 metabolites (M1–M10) were found in human and monkey liver microsomes, eight metabolites (M2, M3, M5, M6, M8, M9, M10, M11) were found in dog liver microsomes, and nine metabolites (M2, M3, M5, M6, M7, M8, M9, M10, M11) were found in rat and mouse liver microsomes. The major in vitro metabolism pathways of zanubrutinib included hydroxylation of the phenoxy phenyl (M5), oxidation and ring opening of the piperidine (M3, M7/M8, M9, M10, M11), epoxidation of ethylene on the acryloyl group (M6), and oxidation of tetrahydropyrazolopyrimidine (M7/M8). M5, the primary metabolite across species, was confirmed as the synthetic standard, BGB-7941. M1, M2, and M4 were minor metabolites from multiple-step oxidations.

3.2 | CYP phenotyping

Potent and selective inhibitors of CYP1A2, CYP2B6, CYP2C8, CYP2C9, CYP2C19, CYP2D6, and CYP3A were used to identify the major enzyme(s) responsible for the metabolism of zanubrutinib and positive controls in HLMs. Following 30-min incubation with HLMs, 32.8% of zanubrutinib remained in the reaction. The addition of the CYP3A inhibitor ketoconazole resulted in 98.9% of zanubrutinib remaining, while the addition of all the other CYP inhibitors produced nearly no effect (Figure 2). When incubated with recombinant CYP enzymes, only rCYP3A4 led to a remarkable disappearance of zanubrutinib (Figure 3).

3.3 | CYP reversible and time-dependent inhibition

The reversible inhibition of zanubrutinib against CYP1A2, CYP2B6, CYP2C8, CYP2C9, CYP2C19, CYP2D6, and CYP3A4 in HLMs is shown in Table 1. K_i was calculated as $IC_{50}/2$, assuming a competitive inhibitory mechanism. In addition, time-dependent CYP inhibition by zanubrutinib was determined by pre-incubation of 10 μM zanubrutinib with HLMs and NADPH for 30 min. Percent loss of enzymatic activity of CYPs was 8.10% for CYP1A2, 15.5% for CYP2B6, 21.9% for CYP2C8, 5.86% for CYP2C9, −14.6% for CYP2D6, −4.58% for CYP2C19, and 19.2% for CYP3A. The activity losses by zanubrutinib were lower than 30% for 7 CYPs, suggesting the potential for zanubrutinib as a clinically relevant time-dependent inhibitor of CYPs is low.[33]

3.4 | CYP induction

Induction of mRNA expression and enzymatic activity of CYP1A2, CYP2B6, CYP3A4, CYP2C8, CYP2C9, and CYP2C19

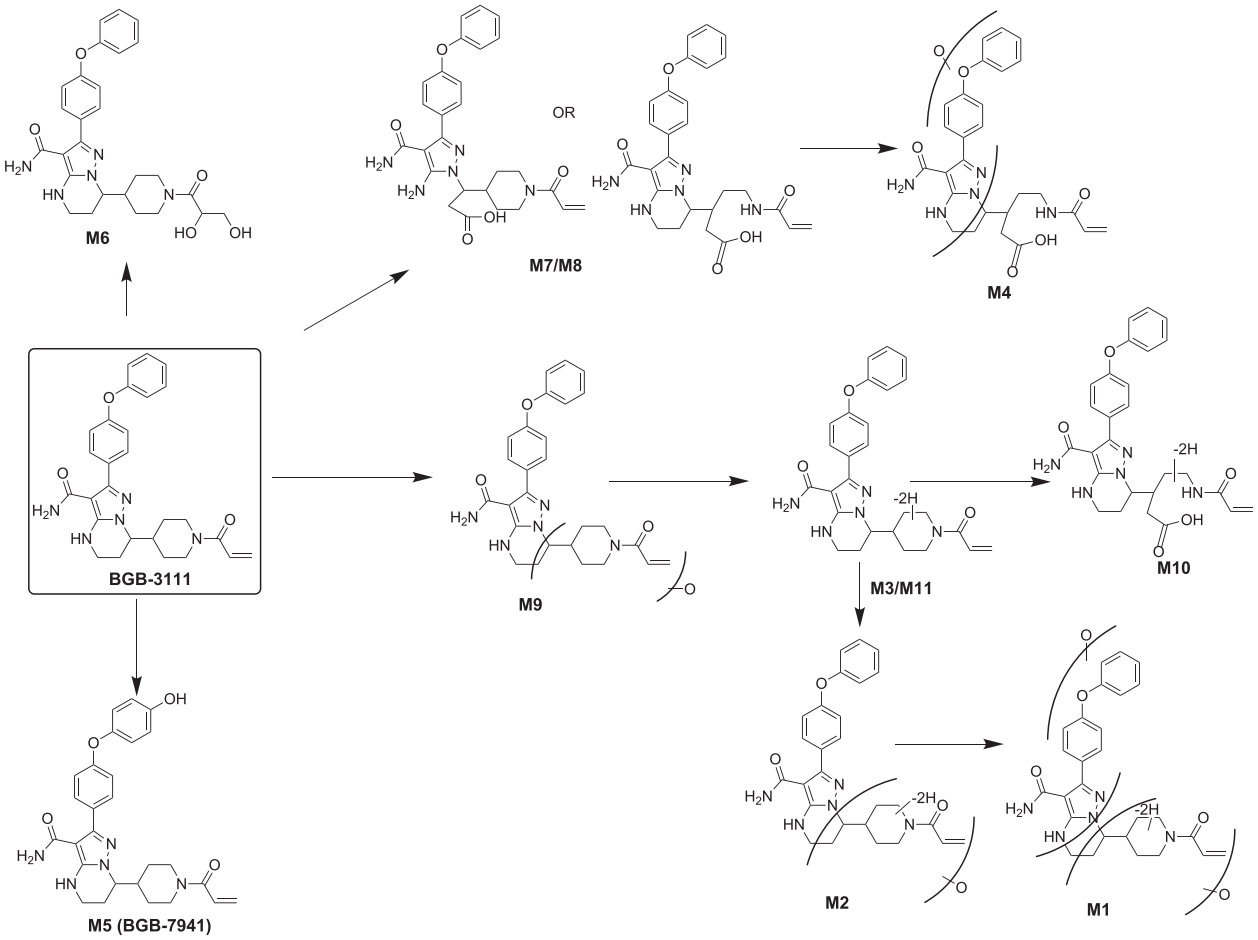

FIGURE 1 Proposed metabolic pathways of zanubrutinib in incubation with different liver microsomes

(enzymatic activity only) in human hepatocytes is presented in Table 2. Zanubrutinib at 0.3, 3, and 30 μM increased CYP3A4 mRNA levels by 3.5-, 13.1-, and 15.0-fold compared with vehicle control, respectively. Zanubrutinib at 3 and 30 μM increased CYP2C8 mRNA levels by 5.0- and 9.8-fold, respectively. CYP1A2, CYP2B6, and CYP2C9 mRNA induction at 0.3–30 μM of zanubrutinib were less than fourfold. Induction of CYP activity was usually less than induction of mRNAs.

3.5 | P-gp substrate and inhibition

The MDCK-MDR1 monolayers in the substrate assay showed intact tight junctions as indicated by minimum permeability for LFY, a low permeability control. An efflux ratio >2 indicates a P-gp substrate.[24] In MDCK-MDR1 cells (Table 3), the efflux ratio of positive control quinidine was 3.10 and was reduced to 0.506 with P-gp inhibitor verapamil. Zanubrutinib (1 μM) exhibited high permeability values. The efflux ratio of zanubrutinib was 3.46 at 1 μM and 2.19 at 10 μM, and reduced to 1.59 at 1 μM and 1.14 at 10 μM in the presence of verapamil. These results revealed that zanubrutinib is a potential P-gp substrate.

In the P-gp inhibition assay with Caco-2 cells, the efflux ratios of digoxin (10 μM) were 16 and 22 with vehicle control. P-gp inhibitor elacridar diminished the efflux ratio of digoxin to 1.1. In the presence of zanubrutinib at 0.5 and 10 μM, the efflux ratios of digoxin were 31 and 17, respectively (Table 3). These results implied that zanubrutinib up to 10 μM was not a significant inhibitor of P-gp.

3.6 | BCRP substrate and inhibition

In BCRP vesicles, an uptake ratio ≥2-fold is indicative of a BCRP substrate.[21] The uptake ratio of LFY, a probe substrate of human BCRP, was 17.4 ± 0.31-fold. The uptake ratios of zanubrutinib at 0.1 and 5 μM were 0.970 ± 0.101-fold and 0.720 ± 0.209-fold, respectively. Zanubrutinib is unlikely to be a substrate of the human BCRP transporter.

In the BCRP inhibition assay, the uptake ratio of LFY in the buffer vehicle was 14.9-fold and was suppressed by the BCRP inhibitor novobiocin by 98.9% (Table 4). Relative BCRP uptake activity of LFY was 93.0%, 108%, 94.5%, and 83.3% of buffer vehicle in the presence of 0.05, 0.2, 1, and 5 μM of zanubrutinib, respectively, suggesting that zanubrutinib at 0.05–5 μM did not inhibit BCRP activity.

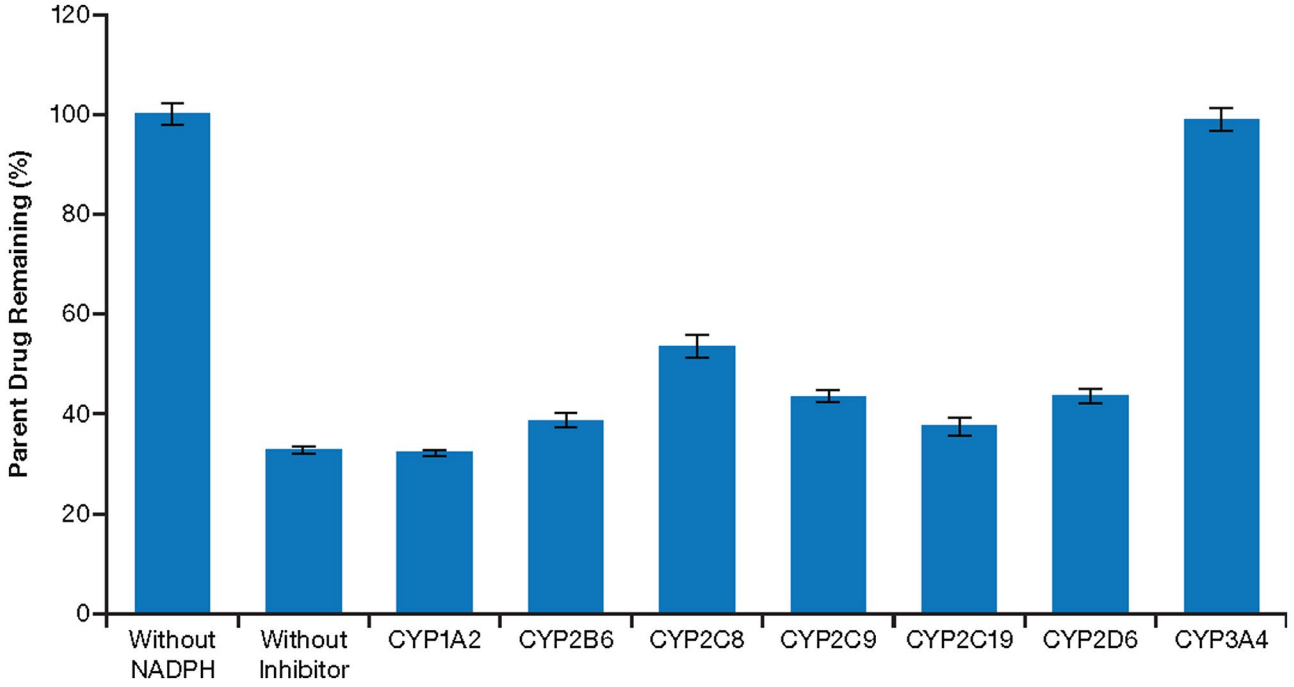

FIGURE 2 Zanubrutinib remaining after incubation in human liver microsomes with chemical inhibitors. Data are the mean (± standard deviation, SD) from triplicate results

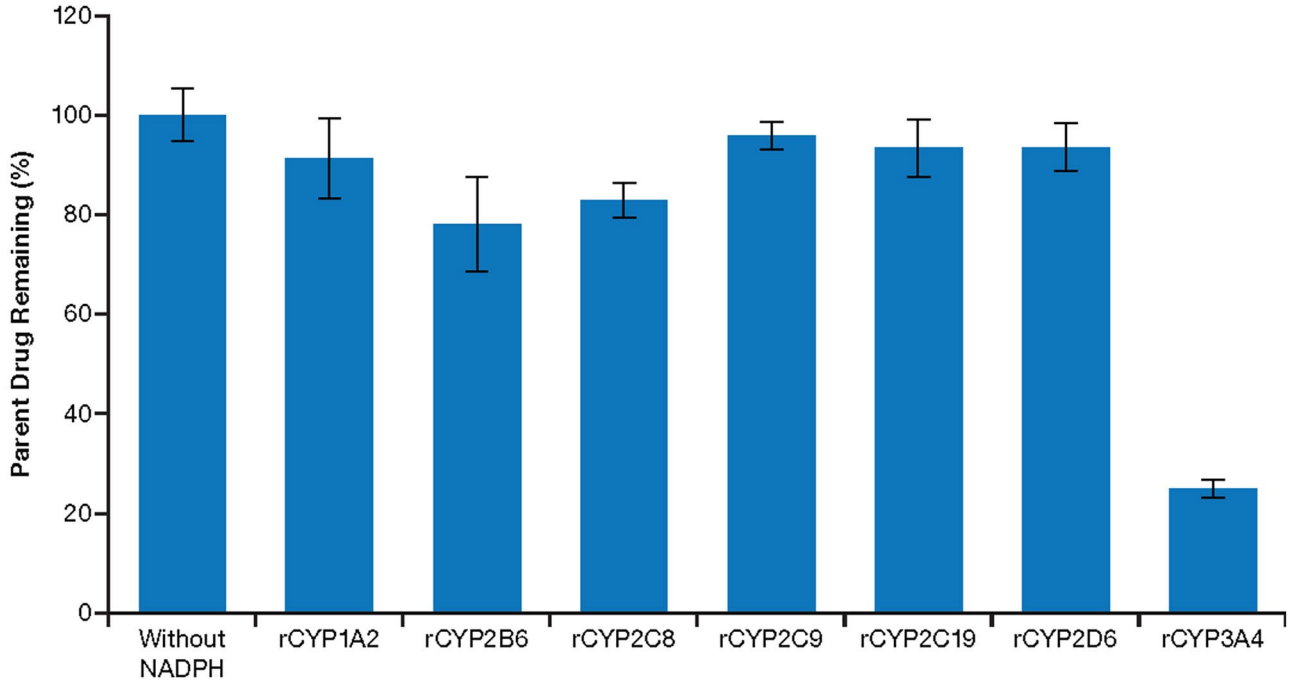

FIGURE 3 Zanubrutinib remaining after incubation in recombinant enzymes. Data are the mean (± standard deviation, SD) from triplicate results

3.7 | Transportation and inhibition of SLC uptake transporters

In SLC transporter overexpressed cells, an uptake ratio ≥2-fold is indicative of a substrate of SLC transporters.[22,24,34] Given the uptake ratios of zanubrutinib at 0.1, 0.3, and 5 μM were <2 (Table 5), zanubrutinib is unlikely to be a substrate of OATP1B1, OATP1B3, OAT1, OAT3, or OCT2.

In the SLC transporter inhibition assays, the uptake activities of the probe substrates were inhibited significantly by the positive

TABLE 1 Evaluation of zanubrutinib as a reversible inhibitor of CYPs in HLMs with estimates of the FDA's value of R_1 and $R_{1,gut}$

Hepatic CYP enzyme	Substrate	IC_{50}† (μM)	K_i(μM)	K_{iu}(μM)	R_1	A_h
CYP1A2	Phenacetin	121	60.5	47.8	1.00	1.00
CYP2B6	Bupropion	121	60.5	47.8	1.00	1.00
CYP2C8	Amodiaquine	4.03	2.02	1.6	1.05	0.95
CYP2C9	Diclofenac	5.69	2.85	2.2	1.04	0.96
CYP2C19	S-Mephenytoin	7.58	3.79	3.0	1.03	0.97
CYP2D6	Dextromethorphan	72.9	36.5	28.8	1.00	1.00
CYP3A	Midazolam	14.3	7.15	5.6	1.00	0.99
	Testosterone	60.6	30.3	23.9	1.00	1.00
Intestinal CYP enzyme	**Substrate**	**IC_{50}† (μM)**	**K_i(μM)**	**K_{iu}(μM)**	**$R_{1,gut}$**	**A_g**
CYP3A	Midazolam	14.3	7.15	5.6	241	0.45
	Testosterone	60.6	30.3	23.9	58	0.77

A_g, term in DDI mechanistic static model for inhibition in gut; A_h, term in DDI mechanistic static model for inhibition in liver; DDI, drug–drug interaction; HLM, human liver microsomes; K_i, reversible inhibition constant; K_{iu}, reversible inhibition constant based on the unbound inhibitor concentration; IC_{50}, half-maximal inhibitory concentration; R_1, DDI basic model value for reversible inhibition; $R_{1,gut}$, DDI basic model value for CYP3A reversible inhibition in gut.

†IC_{50}s were calculated from serial concentrations of zanubrutinib in triplicates (0, 0.274, 0.823, 2.47, 7.41, 22.2, 66.7, and 200 μM).

controls compared to the vehicle (Table 4). The uptake activities of OATP1B1, OATP1B3, OAT1, and OAT3 transporters were not inhibited by zanubrutinib at 0.05–5 μM. For OCT2, activation of OCT2 by zanubrutinib 0.2–1 μM was observed. At 5 μM zanubrutinib, the OCT2-mediated relative activity was 48.4% of vehicle with the IC_{50} estimated to be approximately 4.5 μM.

3.8 | DDI prediction

R_1 and $R_{1,gut}$ of zanubrutinib for reversible inhibition of hepatic and intestinal CYP enzymes, respectively, were estimated in Table 1. Table 6 summarizes E_{max} and EC_{50} of CYP mRNA induction data. The basic kinetic model R_3 was computed from E_{max} and EC_{50}.[27] Table 7 lists the prediction of net DDI effect of CYP inhibition and induction using the mechanistic static model in comparison with clinical data.

4 | DISCUSSION

The studies describe the in vitro metabolism of zanubrutinib, and the investigation of potential for zanubrutinib to be a victim or perpetrator of DDIs via the modulation of metabolizing enzymes or transporters in vitro. The correlations of in vitro and clinical DDIs were explored using basic models and mechanistic static models.

Zanubrutinib presented similar metabolism pathways in human, monkey, dog, rat, and mouse liver microsomes supplemented with NADPH and UDPGA (Figure 1). The primary metabolite M5 in human is expected to be covered in toxicological species rat and dog. All metabolites were oxidative in nature and no direct glucuronide was identified, indicating oxidative metabolism may be responsible for the clearance.

CYP3A is the primary CYP isoform responsible for zanubrutinib metabolism based on phenotyping results using HLMs with selective CYP inhibitors as well as recombinant CYP enzymes. The CYP phenotyping data were subsequently confirmed by a clinical DDI study that showed a 3.8-fold increase in $AUC_{0\text{-inf}}$ of zanubrutinib when co-administered with a potent CYP3A inhibitor (itraconazole) and a 13.5-fold reduction in $AUC_{0\text{-inf}}$ with a potent CYP3A inducer (rifampin).[39] The following clinical results supported that CYP3A-mediated metabolism is mainly responsible for its clearance in humans. The exposure of zanubrutinib could be impacted by CYP3A modulators; therefore, the use of zanubrutinib dosage and co-administered CYP3A modulators should be managed according to the zanubrutinib package insert.[5]

For assessing reversible inhibition of hepatic CYPs, the estimated R_1 (1.05) for hepatic CYP2C8 slightly exceeds the FDA's cutoff value of 1.02, suggesting further modeling or clinical evaluation of CYP2C8-mediated DDI is needed.[24] Due to the high plasma protein binding and thus low projected unbound portal vein concentration I_h, zanubrutinib was predicted to have minimal inhibitory effect on hepatic CYPs. The values of A_h for reversible inhibition of hepatic CYPs tested were estimated to be close to 1 (Table 1). In addition, based on the estimated zanubrutinib I_{gut} (~1360 μM) following 160 mg BID, $R_{1,gut}$ for intestinal CYP3A is higher than the FDA's cutoff value of 11.[24] Additional studies assessing zanubrutinib's inhibition against CYP3A activities are warranted.

Zanubrutinib was initially evaluated for its potential to induce mRNA levels and enzymatic activities of CYP1A2, CYP2B6, and CYP3A4 in human hepatocytes. Due to the induction activity with CYP3A4, induction of CYP2C8, CYP2C9, and CYP2C19 by zanubrutinib was further evaluated in human hepatocytes because both CYP3A4 and CYP2C enzymes are co-induced via PXR activation. The R_3 for average induction fold of CYP3A4 mRNA was estimated as 0.23—well below the FDA's cutoff value of 0.8 (Table 6).

TABLE 2 Average fold induction on CYP1A2, CYP2B6, CYP3A4, 2C8, and 2C9 mRNA and activity over vehicle controls (with vehicle control = 1) in human hepatocytes (N = 3)

Zanubrutinib (μM)	Induction effect	CYP1A2	CYP2B6	CYP3A4	CYP2C8	CYP2C9	CYP2C19
0.3	Fold induction of mRNA level	2.2 ± 0.66	1.6 ± 0.51	3.5 ± 0.61	1.2 ± 0.18	1.1 ± 0.12	NA
3		2.0 ± 0.15	3.6 ± 1.03	13 ± 9.6	5.0 ± 1.5	2.1 ± 0.29	NA
30		3.2 ± 0.93	2.6 ± 0.72	15 ± 10.9	9.8 ± 6.9	3.1 ± 0.59	NA
PCs		82 ± 94	6.4 ± 3.0	28 ± 20	9.0 ± 0.64	3.0 ± 0.48	NA
0.3	Fold induction of activity	1.5 ± 0.31	1.5 ± 0.38	2.0 ± 0.61	1.3 ± 0.22	1.1 ± 0.09	1.2 ± 0.13
3		1.8 ± 0.40	3.7 ± 1.1	6.3 ± 1.4	3.6 ± 0.75	1.5 ± 0.12	1.8 ± 0.27
30		1.4 ± 0.21	1.9 ± 0.67	2.5 ± 0.69	4.7 ± 1.56	1.7 ± 0.31	2.1 ± 0.90
PCs		42 ± 6.4	9.6 ± 5.4	14 ± 4.8	11 ± 4.2	3.4 ± 0.36	5.4 ± 0.75

The fold of induction in hepatocytes of three donors is expressed as mean ± standard deviation. Omeprazole (50 μM) and phenobarbital (1000 μM) served as CYP1A2 and CYP2B6 positive controls, respectively. Rifampin (25 μM) served as CYP3A, CYP2C8, CYP2C9, and CYP2C19 positive control.
NA, not available; PC, positive control.

TABLE 3 Evaluation of zanubrutinib P-gp transportation in MDCK-MDR1 cell line and P-gp inhibition in Caco-2 cell line

Study type	Test article	Cell line	Papp A-B ($\times 10^{-6}$ cm s^{-1})	Papp B-A ($\times 10^{-6}$ cm s^{-1})	Efflux ratio Papp(B-A)/Papp(A-B)
P-gp transportation	Quinidine	MDCK-MDR1	13.1 ± 0.025	40.6 ± 0.13	3.10
	Quinidine + verapamil	MDCK-MDR1	25.8 ± 0.15	13.1 ± 0.14	0.506
	Zanubrutinib 1 μM	MDCK-MDR1	9.16 ± 0.10	31.7 ± 0.12	3.46
	Zanubrutinib 10 μM	MDCK-MDR1	21.9 ± 0.049	47.9 ± 0.094	2.19
	Zanubrutinib 1 μM + verapamil	MDCK-MDR1	17.1 ± 0.12	27.2 ± 0.14	1.59
	Zanubrutinib 10 μM + verapamil	MDCK-MDR1	34.5 ± 0.042	39.4 ± 0.17	1.14
P-gp inhibition	Digoxin	Caco-2	0.700 ± 0.049	15.4 ± 0.40	22
	Digoxin	Caco-2	0.971 ± 0.048	15.8 ± 6.5	16
	Digoxin + elacridar	Caco-2	3.46 ± 0.36	3.81 ± 0.17	1.1
	Digoxin + 0.5 μM zanubrutinib	Caco-2	0.558 ± 0.14	17.2 ± 0.95	31
	Digoxin + 10 μM zanubrutinib	Caco-2	0.852 ± 0.044	14.2 ± 1.60	17

Values expressed as mean ± standard deviation.
A-B, apical-to-basolateral direction; B-A, basolateral-to-apical directions; Caco-2, human colon adenocarcinoma; MDCK, Madin–Darby Canine kidney cells; MDR, multidrug resistance; Papp, apparent permeability coefficient; P-gp, P-glycoprotein.

In addition, the induction of CYP3A4 mRNA was dose dependent. The results indicated that zanubrutinib may cause a clinically relevant induction of CYP3A. However, the dose-dependent induction of CYP1A2 by zanubrutinib was not evident, with a 100-fold increase in zanubrutinib concentration (0.3–30 μM) associated with only a modest increase in the induction of CYP1A2 mRNA. The "flat" induction curve for CYP1A2 mRNA induction, which was <10% of fold induction by the positive control, showed that zanubrutinib is unlikely to be a CYP1A2 inducer. The R_3 of 0.55 for both CYP2B6 and CYP2C8 mRNA induction suggested that zanubrutinib may have a low clinical induction potential for CYP2B6 and CYP2C8. Lower magnitude of CYP2B6 induction than CYP3A4 in vitro and in clinic is noted in literature and a clinical CYP3A DDI study could usually serve as a surrogate for identifying the potential risk for clinical CYP2B6 induction.[40] As for CYP2C induction in human hepatocytes, zanubrutinib presented less than twofold of mRNA induction for CYP2C8 and CYP2C9 mRNA at 0.3 μM ($7 \times I_{max,u}$), but more than twofold of CYP2C8 and CYP2C9 mRNA induction at 3–30 μM. The induction of CYP2C8 and CYP2C9 enzyme activity correlated with induction of mRNA, but at lower levels than mRNA. The marginal twofold induction of CYP2C19 enzyme activity was only visible at 3–30 μM, although mRNA induction data could not be obtained. The current knowledge about in vitro in vivo correlation of CYP2C induction is scarce in the literature.[41,42] Underprediction of clinical CYP2C induction using hepatocyte data has been reported.[41,43,44]

The mechanistic static model was used to predict the net effect of CYP inhibition and induction imposed by zanubrutinib following FDA DDI guidance (Table 7).[24,25] The model demonstrated that CYP3A and CYP2C8 inhibition was overcome by induction. The midazolam induction effect based on induction of CYP3A mRNA by zanubrutinib in human hepatocytes could be significant. The projected induction of CYP2C8 and CYP2B6 built on either CYP mRNA or activity data was low. Zanubrutinib was predicted to have little DDI effect on CYP2C9 substrate warfarin and CYP19 substrate omeprazole (Table 7).

TABLE 4 Inhibitory effects of zanubrutinib on the activity of the efflux transporter BCRP, the hepatic uptake transporters OATP1B1 and OATP1B3, and the renal uptake transporters OAT1, OAT3, and OCT2

		Relative activity (% vehicle) at zanubrutinib concentration (μM)				Positive controls	
Transporter	Substrate	0. 05	0.2	1	5	Compound (μM)	Relative activity (% vehicle)
BCRP	Lucifer Yellow	93 ± 17	108 ± 4.5	94.5 ± 3.5	83.2 ± 2.1	Novobiocin (500 μM)	1.1 ± 0.8
OATP1B1	Estradiol-17β-glucuronide	94.8 ± 2.3	97.9 ± 9.5	87.9 ± 5.7	85.7 ± 6.4	Rifampin (100 μM)	0.93 ± 0.83
OATP1B3	Estradiol-17β-glucuronide	91.6 ± 12	95.2 ± 8.0	97.8 ± 7.1	74.1 ± 10	Rifampin (100 μM)	2.5 ± 2.6
OAT1	p-aminohippuric acid	103 ± 5.6	106 ± 7.8	109 ± 3.9	109 ± 3.3	Probenecid (50 μM)	1.8 ± 0.48
OAT3	Estrone sulfate	90.0 ± 4.2	97.8 ± 7.7	113 ± 27	199 ± 34	Probenecid (50 μM)	12.5 ± 8.0
OCT2	Metformin	107 ± 10	339 ± 5.7	178 ± 36	48.4 ± 5.2	Quinidine (500 μM)	31.5 ± 8.0

The relative activity % of vehicle in the presence of zanubrutinib or positive controls are the means of triplicate results.

BCRP, breast cancer resistance protein; OAT, organic anion transporter; OATP, organic anion transporting polypeptide; OCT, organic cation transporter.

TABLE 5 The uptake ratios of zanubrutinib and positive controls in HEK293 cell lines expressing human OATP1B1, OATP1B3, OAT1, OAT3, and OCT2

Transporters	Zanubrutinib 0.1 μM	Zanubrutinib 0.3 μM	Zanubrutinib 5 μM	Control substrates	
OATP1B1	0.576 ± 0.019	0.773 ± 0.039	1.05 ± 0.036	Estradiol-17β-glucuronide	38.5 ± 5.5
OATP1B3	1.02 ± 0.15	0.977 ± 0.19	1.21 ± 0.14	Estradiol-17β-glucuronide	5.82 ± 0.62
OAT1	0.639 ± 0.19	0.997 ± 0.13	1.04 ± 0.12	p-aminohippuric acid	3.14 ± 0.51
OAT3	0.573 ± 0.044	0.743 ± 0.12	0.892 ± 0.17	Estrone sulfate	16.1 ± 0.45
OCT2	1.84 ± 0.16	1.83 ± 0.23	1.25 ± 0.027	Metformin	3.49 ± 0.26

The uptake rates of zanubrutinib and positive controls were determined in triplicates. The uptake ratio was determined by the ratio of mean uptake rate of a compound in SLC transport overexpressed cells to that in control cell lines.

HEK293, human embryonic kidney 293 cells; OAT, organic anion transporter; OATP, organic anion transporting polypeptide; OCT, organic cation transporter; SLC, solute carrier.

The CYP induction potential of zanubrutinib and the uncertainty in DDI prediction prompted the evaluation of zanubrutinib as a perpetrator for clinical DDI. The probe substrates of CYP3A (midazolam), CYP2C9 (warfarin), and CYP2C19 (omeprazole) were included in a clinical DDI study using a cocktail approach (NCT03561298).[38] As the in vitro DDI properties of zanubrutinib are comparable among CYP2C8, CYP2C9, and CYP2C19 isozymes, and a validated selective CYP2C8 probe is not available in a cocktail study; CYP2C9 and CYP2C19 substrates were selected over a CYP2C8 substrate. The clinical data revealed that coadministration of zanubrutinib reduced the AUCs of CYP3A probe midazolam by 47.5% and CYP2C19 probe omeprazole by 36.5%, suggesting zanubrutinib is a weak inducer of CYP3A and CYP2C19 (Table 7).[45] The clinical induction effect on midazolam was lower than predicted using the mechanistic static model. In human hepatocytes, the fold induction of CYP3A activity was much lower than that of mRNA, thereby the overprediction would be less if induction of CYP3A activity was used over mRNA. However, the bell-shaped activity data with limited zanubrutinib concentrations in human hepatocytes prevented accurate assessments of E_{max} and EC_{50}. In addition, overprediction of clinical CYP3A induction is common since enterocyte concentration, I_g, could be overestimated using the mechanistic static model.[35] The substantial first-pass metabolism and possible binding of zanubrutinib could reduce its effective concentration in enterocytes. The induction effect of zanubrutinib on CYP2C19 probe omeprazole was slightly underestimated by the static model. Induction of CYP3A by zanubrutinib may also play a role in reduction of omeprazole exposure since omeprazole is also a substrate of CYP3A ($f_{m(CYP3A)}$ 0.37).[36] Zanubrutinib had no remarkable effect on the clinical PK of warfarin, in agreement with the static model. Overall, the CYP-based DDI prediction using the static model is in line with clinical data except for CYP3A, a major CYP in intestines.

TABLE 6 Estimates of E_{max}, EC_{50}, and R_3 for CYP mRNA induction by zanubrutinib in three preparations of human hepatocytes

CYP and hepatocyte preparation	E_{max}(fold induction with vehicle control = 0)	EC_{50} (μM)	R_3	C_h	C_g
CYP1A2	3.60	0.29	0.37	N/A	N/A
CYP2B6	2.21	0.73	0.55	1.23	N/A
CYP3A4	17.0	1.75	0.23	1.77	14.6
CYP2C8	10.3	4.89	0.55	1.17	N/A
CYP2C9	3.58	8.64	0.86	1.03	N/A

E_{max} and EC_{50} were estimated from average fold induction values of CYP mRNAs.

C_g, term in DDI mechanistic static model for induction in gut; C_h, term in DDI mechanistic static model for induction in liver; DDI, drug–drug interaction; EC_{50}, concentration supporting half-maximal enzyme induction; E_{max}, maximum fold induction relative to control set to zero; N/A, not available; R_3: DDI basic model value for induction.

TABLE 7 Predictions for clinical DDI studies using mechanistic static models

	Observed AUCR[†,‡] (90% CI)	Observed C_{max} (90% CI)[‡]	Predicted AUCR (mRNA)	Predicted AUCR (activity)
CYP3A4 (midazolam)* F_m =0.88 f_g = 0.57 Ref. [35,36]:	0.525 (0.485–0.569)	0.702 (0.632–0.779)	0.18	N/A
CYP2C9* (S-warfarin) f_m = 0.82 Ref. [37]:	0.998 (0.974–1.02)	0.953 (0.876–1.04)	1.0	1.0
CYP2C19* (omeprazole) f_m = 0.63 Ref. [36]:	0.635 (0.574–0.703)	0.795 (0.65–0.973)	N/A	0.99
CYP2B6 assuming f_m = 1	N/A	N/A	0.82	0.84
CYP2C8 assuming f_m = 1	N/A	N/A	0.90	0.96

$AUC_{0\text{-}t}$, area under the concentration–time curve from time zero to the time of the last quantifiable concentration; AUCR, the ratio of area under the plasma concentration–time curve due to perpetrators; C_{max}, maximum plasma concentration; DDI, drug–drug interaction; F_g, fraction available after intestinal metabolism; F_m, fraction of metabolism by the specific CYP; N/A, not available.

[†]Based on $AUC_{0\text{-}t}$ concentration.

[‡]The observed values are from BGB-3111-108 (NCT03561298).[38]

The transporter assays demonstrated that zanubrutinib is not a substrate of BCRP, OATP1B1, OATP1B3, OCT2, OAT1, and OAT3 (Table 5), but is likely a P-gp substrate (Table 3). However, co-administered P-gp inhibitors would have a limited clinical impact on zanubrutinib absorption due to the high permeability of zanubrutinib across human intestines. Additionally, zanubrutinib is neither a significant inhibitor of P-gp at concentrations up to 10.0 μM nor an inhibitor of BCRP, OATP1B1, OATP1B3, OAT1, and OAT3 up to 5.0 μM, but is a marginal inhibitor against OCT2 (Table 4). The highest concentration of zanubrutinib tested in SLC transporter inhibition assays (5 μM) is roughly 120-fold of $I_{max,u}$ and 94-fold of I_h. The ratio of $I_{max,u}/IC_{50}$ is estimated to be only 0.01 for OCT2, which is lower than the FDA cutoff value of 0.1.[24] Thus, zanubrutinib is unlikely to be a clinically relevant inhibitor of OATP1B1, OATP1B3, OAT1, OAT3, and OCT2. As the maximum concentrations tested in the P-gp and BCRP inhibition assays were considerably less than $0.1 \times I_{gut}$ (~140 μM), concern exists for P-gp or BCRP-mediated clinical DDIs. The potential of zanubrutinib to inhibit P-gp and BCRP transport was evaluated further in the above clinical cocktail DDI study (NCT03561298).[38] Co-administration of zanubrutinib did not significantly affect the exposure of BCRP probe rosuvastatin. Zanubrutinib increased C_{max} of P-gp probe digoxin by 34% but had no significant effect on its AUC. The results support that zanubrutinib has a low impact on P-gp, consistent with in vitro data.

In conclusion, these in vitro studies reveal that the metabolic pathways of zanubrutinib in liver microsomes across species are similar, and its metabolism is mainly mediated by CYP3A. The systemic exposure changes of zanubrutinib inflicted from the coadministration of CYP3A inhibitors and inducers represent the major DDIs with zanubrutinib. Zanubrutinib has a low propensity to cause DDIs through transporter pathways.

ACKNOWLEDGMENTS

The authors wish to acknowledge the investigative center study staff, the study patients, and their families. Editorial assistance was provided by OPEN Health Medical Communications (Chicago, IL) and was funded by BeiGene, Inc.

DISCLOSURE

All authors are employees and own stock in BeiGene, Ltd.

AUTHOR CONTRIBUTIONS

Tang, Zhang, Ou, Su, Sahasranaman, Wang F, and Wang L participated in research design. Tang and Wang F conducted experiments. Tang and Su contributed new reagents or analytic tools. Tang, Zhang, Ou, Su, Sahasranaman, Wang F, and Wang L performed data analysis. Zhang, Ou, Sahasranaman, and Tang wrote or contributed to the writing of the manuscript.

ETHICS STATEMENT

This in vitro cell-free study did not utilize human biospecimens or patient identifiable data; thus, neither approval from the ethics committee nor informed consent was required.

DATA AVAILABILITY STATEMENT

On request, and subject to certain criteria, conditions, and exceptions, BeiGene, Ltd., will provide access to individual de-identified participant data from BeiGene-sponsored global interventional clinical studies conducted for medicines (1) for indications that have been approved or (2) in programs that have been terminated. BeiGene will also consider requests for the protocol, data dictionary, and statistical analysis plan. Data requests may be submitted to DataDisclosure@beigene.com.

ORCID

Heather Zhang https://orcid.org/0000-0003-2445-4528

REFERENCES

1. Ponader S, Burger JA. Bruton's tyrosine kinase: from X-linked agammaglobulinemia toward targeted therapy for B-cell malignancies. *J Clin Oncol*. 2014;32(17):1830-1839.
2. Rickert RC. New insights into pre-BCR and BCR signalling with relevance to B cell malignancies. *Nat Rev Immunol*. 2013;13(8):578-591.
3. Imbruvica. [package insert]. Sunnyvale, CA: Pharmacyclics LLC; 2018.
4. Wang M, Rule S, Zinzani PL, et al. Acalabrutinib in relapsed or refractory mantle cell lymphoma (ACE-LY-004): a single-arm, multicentre, phase 2 trial. *Lancet*. 2018;391(10121):659-667.
5. Brukinsa. [package insert]. San Mateo, CA: BeiGene, Ltd.; 2019.
6. Tam C, Grigg AP, Opat S, et al. The BTK inhibitor, BGB-3111, is safe, tolerable, and highly active in patients with relapsed/refractory B-cell malignancies: initial report of a phase 1 first-in-human trial. *Blood*. 2015;126(23):832.
7. Guo Y, Liu YE, Hu N, et al. Discovery of zanubrutinib (BGB-3111), a novel, potent, and selective covalent inhibitor of Bruton's tyrosine kinase. *J Med Chem*. 2019;62(17):7923-7940.
8. Dimopoulos M, Opat S, Lee H-P, et al. Major responses in MYD88 wildtype (MYD88WT) Waldenstrom macroglobulinemia (WM) patients treated with Bruton tyrosine kinase inhibitor zanubrutinib (BGB-3111). Paper presented at: 24th Annual Congress of the European Hematology Association; June 13-16, 2019; Amsterdam, Netherlands.
9. Konig J, Muller F, Fromm MF. Transporters and drug-drug interactions: important determinants of drug disposition and effects. *Pharmacol Rev*. 2013;65(3):944-966.
10. Song Y, Zhou K, Zou D. Zanubrutinib in patients with relapsed/refractory mantle cell lymphoma. Paper presented at: 15th International Conference on Malignant Lymphoma Palazzo dei Congressi; June 18-22, 2019; Lugano, Switzerland.
11. Calquence. [package insert]. Wilmington, DE: AstraZeneca Pharmaceuticals LP; 2019.
12. Brüggemann R, Alffenaar J-W, Blijlevens N, et al. Clinical relevance of the pharmacokinetic interactions of azole antifungal drugs with other coadministered agents. *Clin Infect Dis*. 2009;48(10):1441-1458.
13. de Jong J, Skee D, Murphy J, et al. Effect of CYP3A perpetrators on ibrutinib exposure in healthy participants. *Pharmacol Res Perspect*. 2015;3(4):e00156.
14. Zydelig. [package insert]. Foster City, CA: Gilead Sciences, Inc.; 2018.
15. Kim RB. Drugs as P-glycoprotein substrates, inhibitors, and inducers. *Drug Metab Rev*. 2002;34(1–2):47-54.
16. Kim RB, Wandel C, Leake B, et al. Interrelationship between substrates and inhibitors of human CYP3A and P-glycoprotein. *Pharm Res*. 1999;16(3):408-414.
17. Burger JA, Tedeschi A, Barr PM, et al. Ibrutinib as initial therapy for patients with Chronic Lymphocytic Leukemia. *N Engl J Med*. 2015;373(25):2425-2437.
18. Alam K, Crowe A, Wang X, et al. Regulation of organic anion transporting polypeptides (OATP) 1B1- and OATP1B3-mediated transport: an updated review in the context of OATP-mediated drug-drug interactions. *Int J Mol Sci*. 2018;19(3):855.
19. Reese MJ, Savina PM, Generaux GT, et al. In vitro investigations into the roles of drug transporters and metabolizing enzymes in the disposition and drug interactions of dolutegravir, a HIV integrase inhibitor. *Drug Metab Dispos*. 2013;41(2):353-361.
20. Livak KJ, Schmittgen TD. Analysis of relative gene expression data using real-time quantitative PCR and the $2^{-\Delta\Delta CT}$ method. *Methods*. 2001;25(4):402-408.
21. Poirier A, Portmann R, Cascais A-C, et al. The need for human breast cancer resistance protein substrate and inhibition evaluation in drug discovery and development: why, when, and how? *Drug Metab Dispos*. 2014;42(9):1466-1477.
22. Kimoto E, Mathialagan S, Tylaska L, et al. Organic anion transporter 2-mediated hepatic uptake contributes to the clearance of high-permeability-low-molecular-weight acid and zwitterion drugs: evaluation using 25 drugs. *J Pharmacol Exp Ther*. 2018;367(2):322-334.
23. Taghikhani E, Fromm MF, Konig J. Assays for analyzing the role of transport proteins in the uptake and the vectorial transport of substances affecting cell viability. *Methods Mol Biol*. 2017;1601:123-135.
24. FDA. In Vitro Drug Interaction Studies. Cytochrome P450 enzyme and transporter mediated drug interactions. *Guidance for Industry*. 2020. https://www.fda.gov/media/134582/download. Accessed July 12, 2021.
25. Cheng Y, Ma L, Chang SY, Humphreys WG, Li W. Application of static models to predict midazolam clinical interactions in the presence of single or multiple hepatitis C virus drugs. *Drug Metab Dispos*. 2016;44(8):1372-1380.
26. Hallifax D, Houston JB. Binding of drugs to hepatic microsomes: comment and assessment of current prediction methodology with recommendation for improvement. *Drug Metab Dispos*. 2006;34(4):724.
27. Kenny JR, Ramsden D, Buckley DB, et al. Considerations from the IQ Induction Working Group in response to drug-drug interaction guidances from regulatory agencies: focus on CYP3A4 mRNA in vitro response thresholds, variability, and clinical relevance. *Drug Metab Dispos*. 2018;46(9):1285-1303.
28. Lineweaver H, Burk D. The determination of enzyme dissociation constants. *J Am Chem Soc*. 1934;56(3):658-666.
29. Ou YC, Liu L, Tariq B, et al. Population pharmacokinetic analysis of the BTK inhibitor zanubrutinib in healthy volunteers and patients with B-cell malignancies. *Clin Transl Sci*. 2021;14(2):764-772.
30. Wang K, Yao X, Zhang M, et al. Comprehensive PBPK model to predict drug interaction potential of zanubrutinib as a victim or perpetrator. *CPT Pharmacometrics Syst Pharmacol*. 2021;10(5):441-454.
31. Harding SD, Sharman JL, Faccenda E, et al. The IUPHAR/BPS Guide to PHARMACOLOGY in 2018: updates and expansion to

encompass the new guide to IMMUNOPHARMACOLOGY. *Nucleic Acids Res*. 2018;46(D1):D1091-D1106.
32. Alexander SPH, Kelly E, Mathie A, et al. The concise guide to pharmacology 2019/20: transporters. *Br J Pharmacol*. 2019;176(Suppl 1):S397-S493.
33. Obach RS, Walsky RL, Venkatakrishnan K. Mechanism-based inactivation of human cytochrome p450 enzymes and the prediction of drug-drug interactions. *Drug Metab Dispos*. 2007;35(2):246-255.
34. Gao C, Huo L, Welsh C, Pham C. Establishment of a complete in vitro drug transporter panel to meet regulatory guidelines (abstract #P241). Paper presented at: 12th International ISSX Meeting; July 28-31, 2019; Portland, OR, USA.
35. Galetin A, Gertz M, Houston JB. Contribution of intestinal cytochrome p450-mediated metabolism to drug-drug inhibition and induction interactions. *Drug Metab Pharmacokinet*. 2010;25(1):28-47.
36. Parmentier Y, Pothier C, Hewitt N, et al. Direct and quantitative evaluation of the major human CYP contribution (fmCYP) to drug clearance using the in vitro Silensomes model. *Xenobiotica*. 2019;49(1):22-35.
37. Siu YA, Lai WG. Impact of probe substrate selection on cytochrome P450 reaction phenotyping using the relative activity factor. *Drug Metab Dispos*. 2017;45(2):183-189.
38. Ou YC, Tang Z, Novotny W, et al. Evaluation of drug interaction potential of zanubrutinib with cocktail probes representative of CYP3A4, CYP2C9, CYP2C19, P-gp and BCRP. *Br J Clin Pharmacol*. 2021;87(7):2926-2936.
39. Mu S, Tang Z, Novotny W, et al. Effect of rifampin and itraconazole on the pharmacokinetics of zanubrutinib (a Bruton's tyrosine kinase inhibitor) in Asian and non-Asian healthy subjects. *Cancer Chemother Pharmacol*. 2020;85(2):391-399.
40. Fahmi OA, Shebley M, Palamanda J, et al. Evaluation of CYP2B6 induction and prediction of clinical drug-drug interactions: considerations from the IQ Consortium Induction Working Group-an industry perspective. *Drug Metab Dispos*. 2016;44(10):1720-1730.
41. Hariparsad N, Ramsden D, Palamanda J, et al. Considerations from the IQ Induction Working Group in response to drug-drug interaction guidance from regulatory agencies: focus on downregulation, CYP2C induction, and CYP2B6 positive control. *Drug Metab Dispos*. 2017;45(10):1049-1059.
42. Nagai M, Hosaka T, Satsukawa M, Yoshinari K. Characterization of CYP2C induction in cryopreserved human hepatocytes and its application in the prediction of the clinical consequences of the induction. *J Pharm Sci*. 2018;107(9):2479-2488.
43. Kirby BJ, Collier AC, Kharasch ED, Whittington D, Thummel KE, Unadkat JD. Complex drug interactions of HIV protease inhibitors 1: inactivation, induction, and inhibition of cytochrome P450 3A by ritonavir or nelfinavir. *Drug Metab Dispos*. 2011;39(6):1070-1078.
44. Machavaram K, Almond L, Crewe K, et al. Evaluation of In Vitro-In Vivo Extrapolation (IVIVE) of the induction potential for known CYP2C9 inducers. Paper presented at: 14th European ISSX Meeting; June 26-29, 2017; Gürzenich Köln, Cologne, Germany.
45. FDA. Clinical Drug Interaction Studies. Cytochrome P450 Enzyme and transporter mediated Drug Interactions. *Guidance for Industry*. 2020. https://www.fda.gov/media/134581/download. Accessed July 12, 2021.

How to cite this article: Zhang H, Ou YC, Su D, et al. In vitro investigations into the roles of CYP450 enzymes and drug transporters in the drug interactions of zanubrutinib, a covalent Bruton's tyrosine kinase inhibitor. *Pharmacol Res Perspect*. 2021;9:e00870. https://doi.org/10.1002/prp2.870